Performance of FMT with Time Confined and Frequency Confined Pulses over Indoor Radio Channels

Nicola Moret, Salvatore D'Alessandro, Andrea M. Tonello
Dipartimento di Ingegneria Elettrica, Gestionale e Meccanica (DIEGM)
Università degli Studi di Udine
Via delle Scienze, 208, 33100 - Udine -Italy
E-mail: {nicola.moret, salvatore.dalessandro, tonello}@uniud.it

***Abstract*—In this paper we study the performance and complexity tradeoff of filtered multitone modulation (FMT) in statistically representative indoor radio channels. We consider two design approaches. The first one is based on the use of long prototype pulses with high sub-channel frequency confinement. The second one follows an orthogonal design with minimal length pulses (down to the length of one transmitted symbol) and good frequency confinement. We present a simulation analysis showing that the FMT system achieves higher capacity than conventional OFDM. This is true also for FMT with minimal length pulses whose complexity is almost comparable to that of orthogonal frequency division multiplexing (OFDM) with an identical number of sub-channels.**

I. Introduction

Filtered multitone (FMT) modulation is a form of multicarrier (MC) transmission [1] that is used for signaling over wide band frequency selective fading channels. More in detail, FMT is a digital realization of multi carrier modulation that deploys uniformly spaced sub-carriers and identical prototype pulses across all the sub-channels. It has been originally proposed for application over broadband wireline channels [2], and subsequently it has also been investigated for wireless [3],[4] and power line [5], [6] applications. Orthogonal frequency division multiplexing (OFDM) can also be viewed as an FMT scheme that deploys rectangular time domain filters.

In general, FMT privileges the sub-channel frequency confinement rather than the time confinement, as for example OFDM does. With frequency confined pulses the sub-channels are quasi-orthogonal to each other minimizing the inter-carrier interference (ICI). The inter-symbol interference (ISI), introduced by the signaling over a frequency selective channel, can be mitigated with sub-channel equalization. We refer to this design approach as frequency confined FMT (FC-FMT). Clearly, the frequency confinement, characteristic of FC-FMT, requires long prototype pulses that may considerably increase the implementation complexity [3],[4],[7],[8].

Another approach to design an FMT system is based on the use of time confined pulses, i.e., it is possible to design a perfectly orthogonal FMT system (with an ideal channel) yet using very short prototype pulses. A method for such a design has been presented in [9]. This method allows the FMT system to deploy minimal length pulses (down to that of one transmitted symbol) that are maximally confined in frequency. We refer to this design approach as time confined FMT (TC-FMT). Clearly, the implementation complexity of TC-FMT is lower than that of FC-FMT.

In this paper, we study the performances of FC-FMT and TC-FMT over typical WLAN channels [10]. We show that FC-FMT that uses long root-raised-cosine pulses yields better performance, in terms of achievable rate, than TC-FMT. However, we discuss the efficient implementation of both schemes and we highlight that FC-FMT has higher implementation complexity. The performances benchmark is done considering OFDM as baseline system. Numerical results show that in many cases OFDM achieves a rate that is lower than that of both FC-FMT and TC-FMT. Furthermore, since TC-FMT uses minimal length prototype pulse, its implementation complexity is very similar to that of OFDM.

The paper is organized as follows. In Section II, we describe the general system model. In Sections III and IV, we briefly recall the FC-FMT and the TC-FMT systems, and in Section V, we analyze their computational complexity. Then, in Section VI, we report numerical results showing the comparison in terms of achievable rate and complexity between FC-FMT and TC-FMT. Finally, in Section VII, the conclusions follow.

II. System Model

We consider a general MC scheme where the high rate discrete-time transmitted signal, at the output of the synthesis filter bank (FB), is obtained by the modulation of M data streams at low rate $a^{(k)}(Nn)$, with $k \in \{0, \cdots, M-1\}$, that belong to a QAM constellation. The transmitted signal can be written as

$$x(n) = \sum_{k=0}^{M-1} \sum_{\ell \in \mathbb{Z}} a^{(k)}(N\ell) g^{(k)}(n - N\ell), \qquad (1)$$

The work of this paper has been partially supported by the European Community's Seventh Framework Programme FP7/2007-2013 under grant agreement n. 213311, project OMEGA - Home Gigabit Networks.

where M is the number of sub-channels, $N = M + \beta$ is the sampling-interpolation factor, with β equal to the overhead (OH) duration in samples. According to (1), the signals $a^{(k)}(Nn)$ are upsampled by a factor N and are filtered by the modulated pulses $g^{(k)}(n) = g(n)W_M^{-kn}$, with $g(n)$ being the prototype filter of the synthesis bank and $W_M^{kn} = e^{-j\frac{2\pi}{M}kn}$. Then, the sub-channel signals are summed and transmitted over the channel.

We use the IEEE 802.11 TGn [10] channel model. This model generates channels belonging to five classes labeled with B,C,D,E,F. Each class is representative of a certain environment, e.g., small office, large open space/office with line of sight (LOS) and non LOS (NLOS) propagation. Both small scale multipath fading and large scale path loss fading as a function of the distance are taken into account. Although the model allows us to consider MIMO channels, we restrict ourselves to the case of single-transmit/single-receive antenna. For a detailed description of the model, see [10].

The received signal $y(n)$ is analyzed with a filter bank having modulated sub-channel pulses $h^{(k)}(n) = h(n)W_M^{-kn}$ with $h(n)$ being the prototype pulse of the analysis bank, and are downsampled by a factor N. Therefore, before equalization, the signal received in the k-th sub-channel is given by

$$b^{(k)}(Nn) = a^{(k)}(Nn)g_{TOT}^{(k)}(0) + ISI^{(k)}(Nn) + ICI^{(k)}(Nn) + \eta^{(k)}(Nn)\,. \quad (2)$$

In (2), $g_{TOT}^{(k)}(0)$ denotes the amplitude of the data of interest, whereas, $ISI^{(k)}(Nn)$, $ICI^{(k)}(Nn)$, and $\eta^{(k)}(Nn)$ respectively denote the ISI, the ICI and the noise term experienced in sub-channel k. The interference terms are in general present when transmitting through a frequency selective channel. They can be mitigated with some form of equalization. The filter bank design aims at reaching a tradeoff between ISI and ICI. While the presence of both ISI and ICI requires a multi-channel equalizer, the presence of only ISI allows us to use sub-channel equalization. In our analysis we consider the use of linear sub-channel equalization only. Therefore, the signal after the sub-channel equalization can be written as

$$b_{EQ}^{(k)}(Nn) = a^{(k)}(Nn)g_{EQ}^{(k)}(0) + ISI_{EQ}^{(k)}(Nn) + ICI_{EQ}^{(k)}(Nn) + \eta_{EQ}^{(k)}(Nn)\,, \quad (3)$$

where we use the subscript EQ to denote the dependence from the equalizer. The terms $g_{EQ}^{(k)}(0)$, $\eta_{EQ}^{(k)}(Nn)$, $ISI_{EQ}^{(k)}(Nn)$ and $ICI_{EQ}^{(k)}(Nn)$, respectively denote the peak of the overall impulse response, the noise term and the interference terms at the k-th sub-channel equalizer output.

In order to evaluate the system performances, we assume parallel Gaussian channels and independent and Gaussian distributed input signals, which render ISI and ICI also Gaussian (cf. e.g. [11]). Therefore, the achievable rate in bit/s for a given channel realization, after sub-channel equalization, is given by

$$C(\beta) = \frac{1}{(M+\beta)T}\sum_{k=0}^{M-1}\log_2\left(1 + SINR_{EQ}^{(k)}(\beta)\right), \quad (4)$$

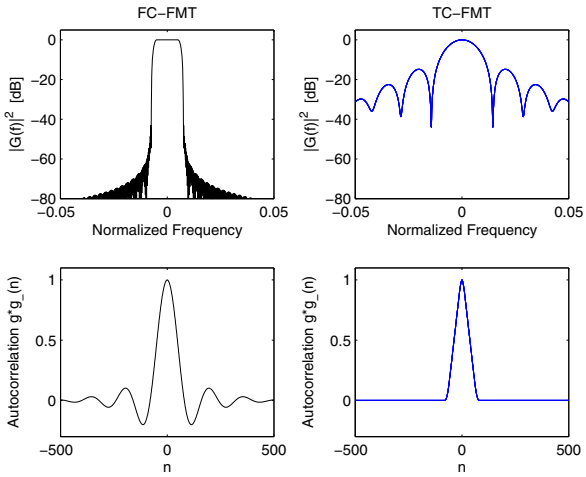

Fig. 1. Examples of frequency response and temporal autocorrelation of FC-FMT and TC-FMT pulses.

where $SINR_{EQ}^{(k)}(\beta)$ denotes the signal over interference plus noise ratio experienced in sub-channel k when we transmit using an overhead of β samples. It is defined as

$$SINR_{EQ}^{(k)}(\beta) = \frac{P_{\mathrm{U},EQ}^{(k)}(\beta)}{P_{\eta,EQ}^{(k)} + P_{\mathrm{I},EQ}^{(k)}(\beta)}, \quad (5)$$

where $P_{\mathrm{U},EQ}^{(k)}(\beta)$, $P_{\mathrm{I},EQ}^{(k)}(\beta)$ and $P_{\eta,EQ}^{(k)}$ respectively denote the useful, the interference, and the noise power terms on sub-channel k after the equalization stage.

Formula (4) shows that the achievable rate is a function of the OH. That is, for each channel realization, the optimal OH can be found as

$$\beta_{opt} = \underset{\beta\in\{0,\ldots,L_{ch}-1\}}{\operatorname{argmax}} \{C(\beta)\}\,, \quad (6)$$

where L_{ch} denotes the channel duration in samples. In (4), T denotes the sampling period.

It is worth noting that all the modulated filter bank schemes can adapt the OH to the channel condition as described by (6). Clearly, the OH adaption increases the implementation complexity. This is because, the achievable rate (4) is not a convex function of the OH and thus the optimal OH has to be found doing an exhaustive search (6).

In the next sections we derive FC-FMT and TC-FMT from the general filter bank scheme.

III. Frequency Confined FMT (FC-FMT)

In FC-FMT the sub-channel symbol period is N and the analysis pulse is matched to the synthesis pulse, i.e., $h(n) = g^{(*)}(-n)$. A distinctive characteristic of FC-FMT is that the prototype pulse is designed to obtain high frequency confinement [2], namely long prototype pulses allow FC-FMT to experience a negligible ICI term. Therefore, the equalization task focuses on canceling the ISI term. This observation justifies our assumption of considering only sub-channel equalization. In Fig. 1, we depict an example of

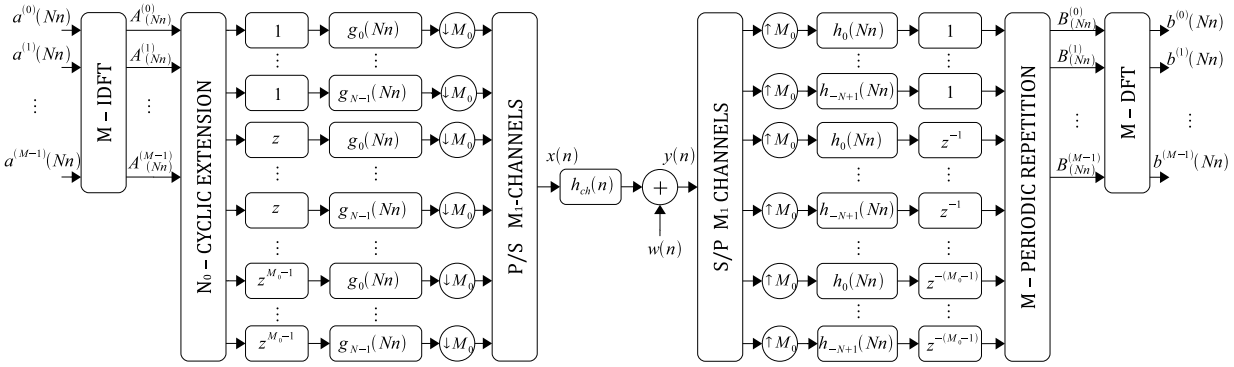

Fig. 2. FMT efficient implementation.

frequency response and temporal autocorrelation for a FC-FMT pulse. More precisely, the pulse for FC-FMT is a root-raised cosine with length $20N$ and roll-off 0.2.

When showing numerical results, for FC-FMT, we consider MMSE fractionally spaced sub-channel equalization [12] with a linear equalizer of 20 taps. Numerical results show that more than 20 taps do not yield significant improvements. Furthermore, we deploy a truncated root-raised-cosine pulse with rolloff equal to $(N-M)/M$ and length $20N$. Clearly, the resulting scheme is complex, but we consider it to report, say, the best attainable performance.

Regarding the choice of the OH (namely $\beta = N - M$), as previously stated, the optimal OH should maximize the achievable rate as in (6). To diminish the computational complexity, in our previous work [13] we have found a limited set of sub-optimal OH values. This set has been found studying the statistics of the optimal OH (6). We have denoted such set as $\mathbb{P}_{FC-FMT} = \left\{\beta^{(99\%)}_{3,FC-FMT}, \beta^{(99\%)}_{10,FC-FMT}, \beta^{(99\%)}_{30,FC-FMT}, \beta^{(99\%)}_{60,FC-FMT}\right\}$, where the subscripts $\{3, 10, 30, 60\}$ denote the distance between transmitter and receiver. The use of the limited set of OH values reduces the OH adaptation to a limited search over the set $\mathbb{P}_{FC-FMT}$, i.e., $\beta_{opt} = \text{argmax}_{\beta \in \mathbb{P}_{FC-FMT}} \{C(\beta)\}$.

IV. Time Confined FMT (TC-FMT)

The TC-FMT scheme can be obtained from the general system model simply substituting the prototype pulse $g(n) = h^*(-n)$ with an FMT orthogonal pulse having minimal length. These pulses satisfy the conditions given by the following system of equations

$$\left[g^{(k)} * h^{(i)}\right](Nn) = \delta_n \, \delta_{i-k}, \quad \forall (k,i) \in \{0, \cdots, M-1\}, \ \forall n \in \mathbb{Z}, \tag{7}$$

where we denote with δ_n the Kronecker delta. Since the solution of the system (7) is not trivial, a significant simplification can be achieved considering MC systems with interpolation-sampling factor $N = (N_0/M_0)M$ with M_0 and N_0 relatively prime integers [9]. We can choose $N_0 = M_0 + 1$ such that we minimize the amount of redundancy, i.e., minimize the ratio $N/M = N_0/M_0$. The solution of this system is not unique, thus, we parameterize the filter coefficients with a minimal set of parameters θ. In order to have maximally frequency confined pulses, we choose pulses that minimize the mean squared error between the pulse spectrum and a target frequency response:

$$\arg\min_{\theta} \int_{-.5}^{.5} |G(f,\theta) - H(f)|^2 df, \tag{8}$$

where $G(f,\theta)$ is the frequency response of the prototype pulse $g(n)$ as function of the parameters θ, and $H(f)$ is the target frequency response. In order to keep low the system implementation complexity, the family of filters adopted in this work has minimal length equal to one symbol duration, i.e., $L_g = N$, where L_g is the prototype pulse length. Furthermore, the interpolation factor is equal to $N = \frac{2^p+1}{2^p}M$. Fig. 1 shows an example of minimal length orthogonal prototype pulse. More details regarding the filter design for TC-FMT are reported in [9].

As for FC-FMT, also for TC-FMT the optimal choice of β should target the achievable rate maximization (4). Due to the fact that the family of filters that we deploy has an OH $\beta = \{M/2^p\}$ with p integer, we limit the OH search over the set $\mathbb{P}_{TC-FMT} = \{M/2^p | \, p = 2, 3, 4\}$. Therefore, the sub-optimal OH is chosen according to $\beta_{opt} = \text{argmax}_{\beta \in \mathbb{P}_{TC-FMT}} \{C(\beta)\}$.

Finally, we notice that when showing numerical results for TC-FMT we use single tap zero forcing sub-channel equalizer.

V. Complexity Comparison

In this section we want to evaluate and compare the computational complexity among the considered FMT schemes. We evaluate the complexity exploiting the efficient implementation scheme presented in [14] and here depicted in Fig. 2. The complexity is measured in complex operations per sample. With reference to Fig. 2, the transmitter comprises the following operations: the data streams $a^{(k)}(Nn)$ are processed by an M-point IDFT block, the output block is cyclically extended to a block of size $M_1 = N_0 M = M_0 N = l.c.m.(M,N)$, and filtered, after a delay, with the N-order polyphase components

of the prototype pulse, e.g., $g_i(Nn) = g(Nn + i)$. Finally, the filter outputs are sampled by a factor M_0 and parallel-to-serial converted. At the receiver side, the received signal is serial-to-parallel converted with a converter of size M_1, the output signals are upsampled by a factor M_0, filtered with the N-order polyphase components of the prototype pulse, e.g., $h_{-i}(Nn) = h(Nn - i)$. Then, after a delay, the periodic repetition with period M of the block of coefficients of size M_1 is applied. Finally, the M-point DFT is performed.

In order to derive a general expression for the computational complexity, we consider for simplicity pulses with length $L = k\,M_1$, with k integer. Thus, the IDFT and DFT blocks have a computational complexity equal to $\alpha\,M\,log_2(M)$, where α takes into account the FFT algorithm used. The cyclic extension and the delays stage do not require any complex operation. Each filter of the polyphase network (PN) has lenght $L_p = L/N$, with L the length of the prototype pulse. If the filter is combined with the sampler with factor M_0, exploiting the polyphase decomposition, the total number of operations is $(2L_p - 1)/M_0$. Otherwise, if the filter is combined with the up-sampler with factor M_0, the complexity becomes $(2L_p - M_0)/M_0$ [15]. Each PN deploys M_1 parallel branches. Thus, the total operations for the synthesis PN is $M_1\,(2L_p - 1)\,/\,M_0$, and for the analysis PN is $M_1\,(2L_p/M_0 - 1)$. Finally, the periodic repetition block requires M_1 operations. The total number of operations per sample for the synthesis and analysis stages is the order of:

$$\frac{(\alpha\,M\,\log_2(M)\,+\,2L)}{N}. \tag{9}$$

Considering the TC-FMT scheme and taking into account that the prototype pulse has length $L = N$ and only 2β coefficients of the prototype pulse differ from a constant, (9) can be simplified into $(\alpha M \log_2 M + 2\beta)\,/N$.

Since OFDM deploys a constant rectangular pulse, its complexity is equal to $(\alpha M \log_2 M)\,/N$.

As an example for a system with $\alpha = 1.2$, M=64 and N=80, the complexity is equal to $\{45.76; 6.56; 5.76\}$ for FC-FMT with filter length $L = 20N$, TC-FMT, and OFDM respectively.

VI. Numerical Results

To obtain numerical results, we have chosen the following system parameters that are essentially those of the IEEE 802.11 standard [16]. The MC system uses $M = 64$ sub-channels with a transmission bandwidth of $20\,MHz$. The signal is transmitted with a constant power spectral density (PSD) of $-53\,dBm/Hz$. At the receiver side, we add white Gaussian noise with PSD equal to $-168\,dBm/Hz$. Thus, the SNR, without path loss and fading, on each sub-channel is $115\,dB$. To show the performance of both FC-FMT and TC-FMT, we use an OFDM baseline system which deploys a fixed CP of $0.8\,\mu s$ ($\beta = 16$ samples), that is the value of CP employed in the IEEE 802.11 standard [16].

Fig. 3 shows the complementary cumulative distribution function (CCDF) of the achievable rate (4) obtained using

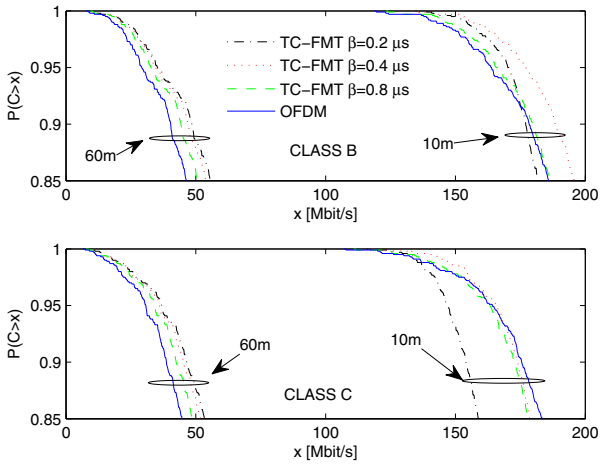

Fig. 3. Achievable rate CCDFs obtained using TC-FMT with different prototype pulses and OFDM. The employed channel classes are the B and C. The distance between transmitter and receiver is set to 10 m and 60 m.

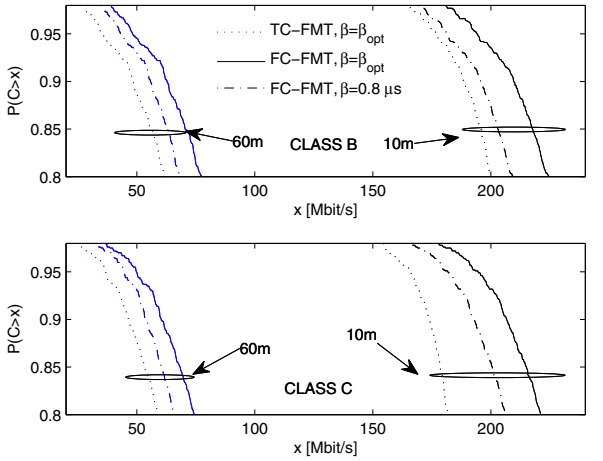

Fig. 4. Achievable rate CCDFs obtained using TC-FMT and FC-FMT with optimized OHs and FC-FMT with fixed OH equal to $0.8\,\mu s$. The employed channel classes are the B and C. The distance between transmitter and receiver is set to $10\,m$ and $60\,m$.

TC-FMT with OH factors $\beta = \{0.2, 0.4, 0.8\}\,\mu s$ and the baseline OFDM system. For the sake of readability, we only show results for channel classes B and C, and for distances between transmitter and receiver equal to $10\,m$ and $60\,m$. More results for OFDM can be found in [13]. From Fig. 3 we observe that the optimal TC-FMT OH factor depends on the distance between transmitter and receiver. In fact, we see that for distances of $60\,m$ and $10\,m$, the optimal OH factor equals $0.2\,\mu s$ and $0.4\,\mu s$ respectively. This behavior is simply explainable observing that when we increase the distance, the path loss increases or equally the SNR decreases. In such a case, the noise dominates on the interference term (see (5)). It follows that a long pulse is useless because it would only decrease the achievable rate (see (4)) without increasing the

SINR. On the contrary, when the distance is short, the SNR is high and thus the interference dominates on the noise. In such a case is important to reduce the interference and thus to use long pulses.

From Fig. 3, we can also observe that TC-FMT outperforms the OFDM baseline system. More precisely, with probability 0.95, the use of TC-FMT gives a gain in achievable rate of 20% and 21% respectively for channel classes B and C when the distance equals $60\,m$. Whereas, when the distance equals $10\,m$, the gain is equal to 8% and 1% for channel classes B and C respectively.

Fig. 4 shows the achievable rate CCDF obtained using TC-FMT and FC-FMT both with optimized OH, and FC-FMT with fixed OH equal to $\beta = 0.8\,\mu s$. The OHs are optimized doing the limited search over the sets $\mathbb{P}_{TC-FMT} = \{0.2, 0.4, 0.8\}\ \mu s$ (see Section IV), and $\mathbb{P}_{FC-FMT} = \left\{\beta^{(99\%)}_{10,FC-FMT} = 0.5\,\mu s, \beta^{(99\%)}_{60,FC-FMT} = 0.2\,\mu s\right\}$ (see Section III). The used channel classes are the B and the C, and the distances between transmitter and receiver are equal to $10\,m$ and $60\,m$. As we can see, FC-FMT with optimized OH that deploys sub-channel equalization outperforms both FC-FMT with fixed OH and TC-FMT. More precisely, with probability equal to 0.95, FC-FMT with optimal OH outperforms TC-FMT by 37% and 35.3% at $60\,m$, and by 10% and 17% at $10\,m$ for channel classes B and C respectively. On the other side, FC-FMT with fixed OH outperforms TC-FMT by 21% and 21.5% at $60\,m$ and by 3% and 9.5% at $10\,m$ for channel classes B and C respectively. Clearly, the improvement given by the use of FC-FMT is paid in terms of computational complexity. In fact, as explained in Section V, FC-FMT substantially increases the complexity w.r.t. TC-FMT.

VII. Conclusions

We have analyzed the performance of two different classes of filtered multitone modulation, one that uses frequency confined pulses (FC-FMT), and the other one that uses time confined orthogonal prototype pulses (TC-FMT). We have shown that over typical WLAN channels both FMT systems outperform the OFDM scheme used in the WLAN standard. Furthermore, the simulations show that if we can afford increased computational complexity, FC-FMT provides significant gains in terms of achievable rate, w.r.t. both TC-FMT and OFDM.

References

[1] J.A.C. Bingham, "Multicarrier Modulation for data Transmission, an Idea whose Time Has Come," *IEEE Commun. Magazine*, vol. 31, pp. 5-14, May 1990.

[2] G. Cherubini, E. Eleftheriou, S. Olcer, "Filtered Multitone Modulation for Very High-Speed Digital Subscribe Lines," *IEEE J. Sel. Areas in Commun.*, pp. 1016-1028, Jun. 2002.

[3] A. M. Tonello, "Performance Limits for Filtered Multitone Modulation in Fading Channels," *IEEE Trans. Wireless Commun.*, vol. 4, no. 5, pp. 2121-2135, Sep. 2005.

[4] A. M. Tonello, "Analytical Results About the Robustness of FMT Modulation with Several Prototype Pulses in Time-Frequency Selective Fading Channels," *IEEE Trans. Wireless Commun.*, vol. 7, no. 5, pp. 1634-1645, May 2008.

[5] F. Pecile, A. M. Tonello, "On the Design of Filter Bank Systems in Power Line Channels Based on Achievable Rate," *in Proc. of IEEE Int. Sym. on Power Line Communications and its Applications (ISPLC 2009)*, Dresden, Germany, Mar. 2009.

[6] A. M. Tonello and F. Pecile, "Efficient Architectures for Multiuser FMT Systems and Application to Power Line Communications," *IEEE Trans. on Commun.*, vol. 57, no. 5, pp. 1275-1279, 2009.

[7] W. Kozek, A.F. Molisch, "Nonorthogonal Pulseshapes for Multicarrier Communications in Doubly Dispersive Channels," *IEEE J. Sel. Areas Commun.*, vol. 16, no. 8, pp. 1579-1589, Oct. 1998.

[8] M. Harteneck, S. Weiss, W. Stewart, "Design of Near Perfect Reconstruction Oversampled Filter Banks for Subband Adaptive Filters," *IEEE Trans. on Circuits and Systems Part II: Analog and Digital Signal Processing*, 46 (8). pp. 1081-1086. ISSN 1057-7130, Aug. 1999.

[9] N. Moret, A. M. Tonello, "Design of Orthogonal Filtered Multitone Modulation Systems and Comparison among Efficient Realizations," *EURASIP Journal on Advances in Signal Processing*, 2010.

[10] V. Ercegl, L. Shumacher et al, IEEE P802.11 Wireless LANs, TGn Channel Models, doc.: IEEE 802.11-03/940r4, May 10, 2004.

[11] J. Seoane, S. Wilson, and S. Gelfand, "Analysis of Intertone and Interblock Interference in OFDM when the Length of the Cyclic Prefix is Shorter than the Length of the Impulse Response of the Channel," *in Proc. of IEEE Global Telecomm. Conf. (GLOBECOM 1997)*, Phoenix, USA, Nov. 1997.

[12] J. Proakis, Digital Communications, chapter 10, fourth edition, Mc Graw Hill.

[13] S. D'Alessandro and A. M. Tonello, "Adaptive Filter Bank Modulation for Next Generation Wireless In-Home Networks," *in Proc. of ICST MOBILIGHT 2010*, Barcelona, Spain, May 2010.

[14] A. M. Tonello, "Time Domain and Frequency Domain Implementations of FMT Modulation Architectures," *in Proc. of IEEE ICASSP 2006*, Toulose, France, May 2006.

[15] Web site: https://ccrma.stanford.edu/~ jos/sasp/N_Channel _Polyphase_Decomposition.html, last visited, Feb. 2010.

[16] IEEE Std.802.11, "Wireless LAN Medium Access Control and Physical Layer Specification," Jun. 2007.